Creating a Stability Lobe Diagram

Jianping Yue
Division of Engineering Technologies and Computer Sciences
Essex County College
Newark, New Jersey
yue@essex.edu

Abstract

Machine tool chatter causes machining instability, surface roughness, and tool wear in metal cutting processes. A stability lobe diagram based on regenerative chatter theory is an effective tool to predict and control chatter. Stability diagrams can be applied in machining processes to optimize the maximum depth of cut at the highest available spindle speed, thus improving the material removal rate and increasing productivity. A stability lobe diagram is formed by a series of intersected scallop-shaped borderlines of stability. The intersections of the lobes denote the deepest stable cuts at various ranges of spindle speed. These optimum depths of cut have traditionally been found by graphical solution from the stability lobe diagram. The creation of a stability lobe diagram requires lengthy procedures and calculations. Furthermore, discussion of the topic in manufacturing textbooks is still limited. This paper presents a simple method to analytically calculate the approximate optimum depths of cut and determine the corresponding spindle speeds. This method allows machine operators to practically choose cutting parameters, instructors to effectively teach the regenerative chatter theory, and students to easily create stability lobe diagrams and practice optimizing cutting parameters. A procedure is also introduced to use a spreadsheet to analyze machining parameters and construct stability lobe diagrams. The characteristics and limitations of the stability lobe diagram are discussed. Case studies are also provided to illustrate the method and verify the results.

1. Introduction

Machining by metal cutting is one of the most popular manufacturing techniques. Over $100 billion is spent annually on machining operations in the United States [1]. High material removal rate (MRR) and surface quality are always the primary objectives of machining operations. Since the 19th century Industrial Revolution, continuous improvements have been made in machine tools and cutting tools. New materials and designs have significantly increased the hardness and life of cutting tools. High-speed machining centers can now operate at spindle speeds as high as half a million revolutions per minute (RPM). In order to utilize the power and capacity of these new machine tools and cutting tools, and to achieve potential high MRR and desired surface quality, optimum machining parameters are necessary.

Much research has been done on improving the material removal rate and surface quality by setting optimal machining parameters and controlling machine tool chatter. Machine chatter theory was first developed by Tobias & Fishwick [2] in the late 1950s. For half a century, many researchers have contributed to the development of the regenerative chatter theory, including Merritt [3], Tlusty [4, 5], Smith [6], and Altintas & Budak [7]. Regenerative chatter theory creates a relationship between spindle speed and the critical chip width or depth of cut. The theory produces a stability lobe diagram and makes it possible to achieve the highest applicable MRR for a machining process. In the past decade, there have been more than a dozen doctoral dissertations [8-24] and a number of research articles published [25-75]. Most of these recent researches have focused on topics such as multimode chattering, variations of machine tools and cutting tools, numerical modeling, and instrumental measurements. However, a thorough discussion of chatter theory and equations, along with improvement to techniques for creating the stability lobe diagram, are equally important. In particular, they are valuable in the classroom, so that students can easily create a stability lobe diagram and practice optimizing cutting parameters. Manufacturing industries can also apply the theory by using practical and simplified techniques to improve MRR and production rate. A method is presented below to create the stability lobe diagram using a spreadsheet. It also presents an analytical rather than graphical method of calculating the approximate optimal chip widths.

2. Governing equations of machine chattering

The governing equations of machine chattering can be derived from the general equation of vibration and the regenerative chatter equations.

2.1 Critical chip width

In orthogonal cutting, the cutting force F is proportional to the cutting area (the product of the chip width or depth of cut b and thickness h) [3]:

$$F = k_s\, b\, h = k_s\, b\, [x(t - T) - x(t)] \tag{1}$$

where k_s is the cutting stiffness or specific power, x is the displacement of the cutter normal to the cut, t is time, and T is the time interval between the previous and current cuts. Substituting eq. 1 into the general equation of vibration:

$$m\ddot{x} + c\dot{x} + kx = F \tag{2}$$

We obtain the formula for chip width [4]:

$$b = \frac{-1}{2k_s G_R} \tag{3}$$

where G_R is the real part of the frequency response function (FRF) G as in the standard solution of eq. 2 alone,

$$\frac{x}{F} = \frac{1-r^2}{k[(1-r^2)^2 + (2\zeta r)^2]} + i\frac{-2\zeta r}{k[(1-r^2)^2 + (2\zeta r)^2]} = G_R + iG_I = G \tag{4}$$

The reader is directed to standard mechanics textbooks for detailed derivations and solutions for the general equation of vibration.

In eq. 2, eq. 3, and eq. 4:

m = Mass
c = Damping coefficient
k = Stiffness ($k = F / x$)
r = Ratio of chatter frequency to natural frequency ($r = f / f_n$). The natural frequency f_n of the machining system is also called the modal frequency.
ζ = Ratio of the damping coefficient to the critical damping coefficient ($\zeta = c / c_c$). The critical damping coefficient $c_c = 2\sqrt{km}$.

When we solve eq. 1 and eq. 2 together, the chip width b is dependent on the frequency f of machine vibration or chatter through the frequency ratio r. For each chatter frequency generated on a machining system, there is a corresponding critical chip width b. The cutting process is stable when its chip width is less than the critical value and unstable otherwise.

2.2 Minimum chip width

The chip width b should always be positive (greater than or equal to zero.) Therefore, from eq. 3 and eq. 4, the minimum chip width b_{min} occurs at the maximum negative value of G_R (or true minimum $G_{R,\,min}$,) when $r = \sqrt{1+2\zeta}$ [4]:

$$b_{\min} = \frac{-1}{2k_s G_{R,\min}} = \frac{2k\zeta(1+\zeta)}{k_s} \tag{5}$$

This minimum chip width represents a limit in a machining process. Since it is independent of the chatter frequency, there is only a fixed value determined by the materials and geometries of the cutter and the workpiece. A cutting process is unconditionally stable when the chip widths are under this critical value. A dimensionless chip width may be represented by the ratio of chip width to the minimum chip width [5]:

$$r_b = \frac{b}{b_{\min}} = \frac{G_{R,\min}}{G_R} = \frac{(1-r^2)^2 + (2\zeta r)^2}{-4\zeta(1+\zeta)(1-r^2)} \tag{6}$$

Eq. 3 represents the relationship between the chip width b and chatter frequency f ($f = r f_n$). While eq. 6 represents the relationship between the dimensionless chip width ratio r_b and chatter frequency ratio r.

2.3 Equations of regenerative chatter

Roughness or waviness always exists on the machined surface of workpieces due to vibrations. According to regenerative chatter theory, chatter occurs whenever there is a shift of the phase angle ε between the current and previous surface waviness. Therefore, the ratio of chatter frequency f to tooth-stroke frequency f_t represents the number of surface waves between consecutive cutter teeth, and can be written as an integer n (also called the lobe number. n = 0, 1, 2, …) plus a fraction of $\varepsilon / 2\pi$ radians [5]:

$$\frac{f}{f_t} = \frac{r}{r_t} = n + \frac{\varepsilon}{2\pi} \tag{7}$$

where r_t is the ratio between the tooth frequency and natural frequency ($r_t = f_t / f_n$). The phase shift angle ε between the current and previous surface waviness may be expressed as [5]:

$$\varepsilon = \pi + 2\tan^{-1}\frac{G_I}{G_R} \tag{8}$$

Since the real and imaginary FRF's G_R and G_I are both negative (eq. 4), using the principal range of $-\pi/2 < tan^{-1}x < \pi/2$, we have $0 < tan^{-1}(G_I / G_R) < \pi/2$, and the phase shift angle ε is between $\pi < \varepsilon < 2\pi$.

Substitute eq. 3 into eq. 8, and then into eq. 7, we obtain the equation of regenerative chatter:

$$\frac{f}{f_t} = \frac{r}{r_t} = n + \frac{1}{2} + \frac{1}{\pi}\tan^{-1}\frac{-2\zeta r}{1-r^2} \tag{9}$$

Eq. 9 represents the relationships among the chatter frequency f (or r), the tooth frequency f_t (or r_t), and the lobe number n. Together with eq. 3 (or eq.6), they form the governing relationship between the chip width b and spindle speed N, or between the dimensionless chip width ratio r_b and chatter frequency ratio r_t. The spindle speed N can be related to the tooth frequency f_t ($f_t = n_t N / 60$), where n_t is the number of teeth on the cutter.

For multiple-teeth cutters and multiple degrees of freedom, additional parameters and equations are necessary. It has also been observed both theoretically and practically that the relationships represented by the machine chattering equations do not hold for machining processes with very low spindle speeds. Tobias and Fishwick [2] derived equations under different conditions in the low-speed range. These topics are beyond the scope of our discussion.

3. The stability lobe diagram

From eq. 3 and eq. 9, we can create a stability lobe diagram between the chip width b and spindle speed N (Figure 1). We may also create a stability lobe diagram between the dimensionless $r_b = b / b_{min}$ and $r_t = f / f_t$ from eq. 6 and eq. 9 (Figure 2). The dimensionless stability lobe diagram has the advantage of allowing comparisons among different machining conditions. Mixed dimensions are also possible, such as $b \sim r_t$ and $r_b \sim N$, but not recommended.

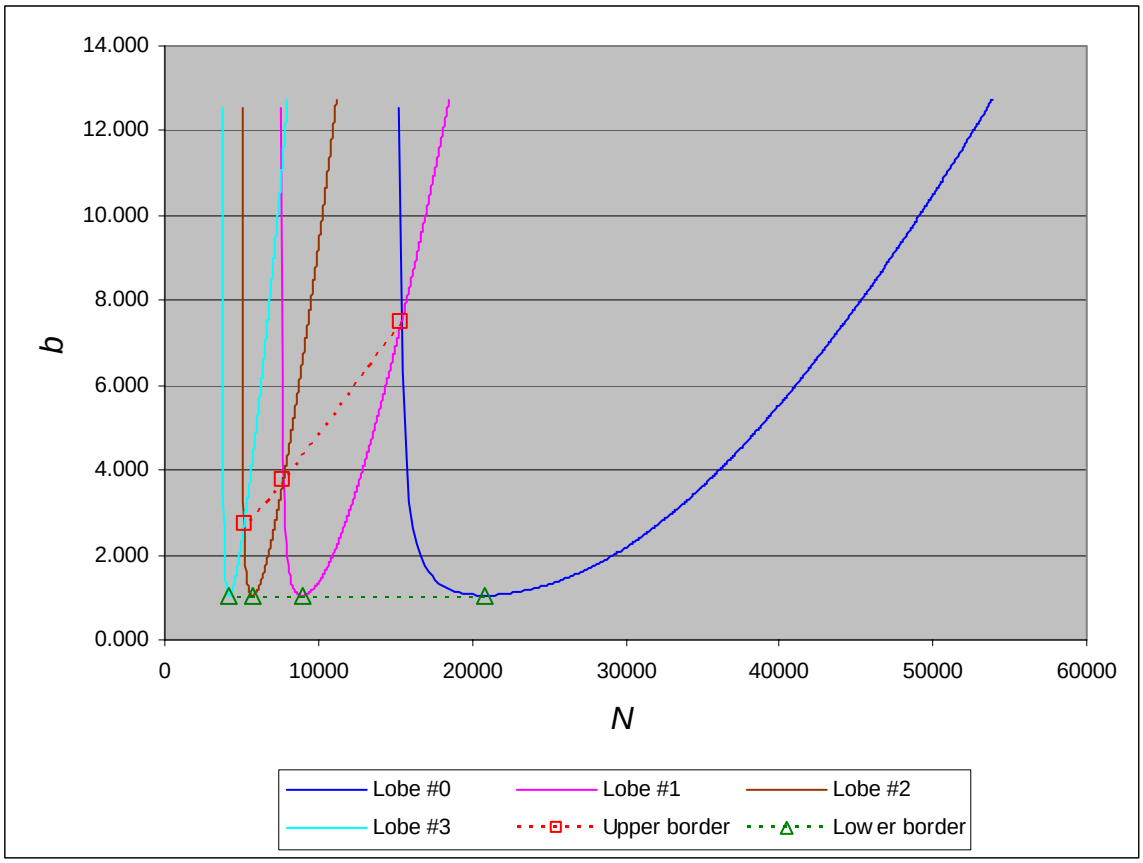

Figure 1 Stability lobe diagram for the prediction of the maximum chip width

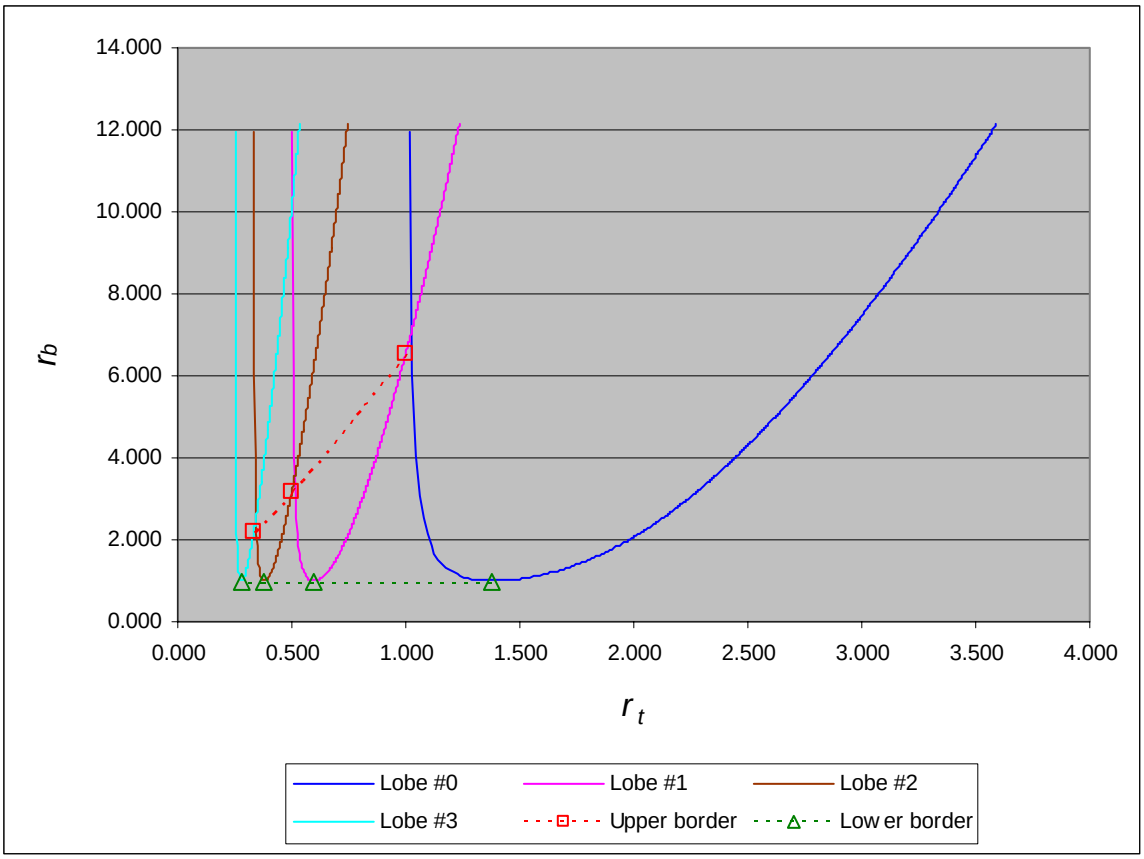

Figure 2 Stability lobe diagram (dimensionless)

Since the series of relationship curves in Figure 1 and Figure 2 are shaped like lobes, the graph is usually called a stability lobe diagram. A stability lobe diagram shows the relationship between chip width (or depth of cut) and spindle speed, with the lobe number as a parameter. Usually, the variable on its x-axis is represented as spindle speed N, tooth frequency f_t ($f_t = n_t N / 60$), or the tooth frequency ratio r_t ($r_t = f_t / f_n$); the variable on its y-axis is represented as chip width b or the chip width ratio r_b ($r_b = b / b_{min}$). The dimensionless relationship of $r_b \sim r_t$ will be discussed. The lobes and their characteristics are similar for the other variables.

It is more convenient to calculate the points on the lobes using spreadsheet software. The step-by-step procedure for generating the points is illustrated in Table 1.

Table 1 Calculating the stability lobes of $r_b \sim r_t$

j	f_j	r_j	r_{bj}	r_{tjn}				
				$n = 0$	$n = 1$	$n = 2$	$n = 4$	…
1	251	1.004	6.026	1.026	0.506	0.336	0.252	…
2	252	1.008	4.061	1.053	0.513	0.339	0.253	…
3	253	1.012	2.135	1.081	0.519	0.342	0.255	…
4	254	1.016	1.678	1.108	0.526	0.345	0.256	…
…	…	…	…	…	…	…	…	…

Step 1. For each increment j of the chatter frequency f_j, calculate r_j and r_{bj} from eq. 6.
Step 2. For each lobe number n, calculate its corresponding r_{tjn} from eq. 9.
Step 3. The points for each n value are plotted to form a single lobe, and a series of lobes (n = 0, 1, 2, …) are plotted to form the stability lobe diagram of $r_b \sim r_t$.

In Table 1, the subscript j indicates the chatter frequency f after the j^{th} increment. The procedure to create the stability lobes of $b \sim N$ is the same as that of $r_b \sim r_t$, except that eq. 3 is used to calculate b instead of using eq. 6 to calculate r_b, and the spindle speed N ($N = 60 f_t / n_t = 60 r_t f_n / n_t$) is used instead of r_t. The results in Table 1 are generated using the same data as the example in Tlusty [4]. The parameters are: $k = 10$, $k_s = 1$, $\zeta = 0.05$, $n_t = 1$, and $f_n = 250$ Hz.

4. Properties of the stability lobe diagram

Some interesting characteristics exist in the stability lobe diagram, which may be utilized to optimize the chip width or depth of cut and obtain the maximum material removal rate (MRR) in machining processes.

4.1 Stability criteria and chatter lines

In a stability lobe diagram, a series of scallop-shaped lobes intersect with each other. These lobes form the limits for chattering. Locally, for each lobe, it is stable below the lobe, and unstable above the lobe. Since the lobes intersect, a point located below one lobe could be above the neighboring lobe. This point must be treated as unstable. Therefore, globally, we must consider the relationship between adjacent lobes in determining stability. The upper portions of any two adjacent lobes above their intersection point should be trimmed off. The intersection points connect all the lobes into "chained" chatter lines (Figure 1.) All the points above the chatter lines are unstable, and below are stable. As spindle speed increases, the lobes become wider with larger intervening spaces between consecutive lobes, and intersection points are higher. This phenomenon creates a desirable situation for machining at both higher speed and deeper cut simultaneously, as well as at a wider speed range.

The two sides of the series of lobes have some special characteristics. The first lobe #0 on the right of the diagram has the maximum stable chip width at its intersection with lobe #1. The right branch of lobe #0 has no intersection with other lobes, which allows unlimited chip width at extremely high spindle speed. Due to the limits of cutter material composition and available motor power, we may not be able to reach the range practically. However, further investigation is needed to verify its theoretical validity. The lobes on the left of the diagram are crowded both horizontally and vertically. The lobes not only become closer together toward the left, but their intersection points also move downward, closer to the minimum chip width (or $r_b = 1$). However, in real machining processes, bigger chip widths or deeper cuts have been reached without chattering. To solve this problem, Tobias and Fishwick [2] derived a different equation that produces a chatter line with bigger chip width.

4.2 The stability regions and their border lines

The entire range of the stability lobe diagram may be divided by the lower and upper border lines (the dashed lines on Figure 1 and Figure 2) into three regions of stability: unconditionally stable, conditionally stable, and unconditionally unstable. The lowest points on the lobes are the minimum chip widths with the same values ($b = b_{min}$ at $r_b = 1$). A horizontal border line can be formed by connecting the lowest points on the lobes or simply drawn at $b = b_{min}$. The region below this line is unconditionally stable, which is independent of chatter frequency or spindle speed. We may also fit a curve through or simply connect all intersection points of the lobes to form another border line. The region above this upper border line is unconditionally unstable, and chatter always occurs in the region. The region in between the two regions is conditionally stable. In the conditionally stable region, points are stable when they are below the lobes, and unstable above the lobes. The upper and lower border lines converge to a point of minimum chip width at $r_b = 1$ when the spindle speed approaches zero.

The division into three stability regions with the two border lines provides a distinctive separation between stable and unstable zones. This enables a quick estimate and selection of the allowable chip width for a machining process to prevent chattering, instead of fine tuning the optimum chip width in the conditionally stable region. We can always safely control the cutting in the unconditionally stable region at all ranges of speeds by limiting the chip width to be smaller than b_{min}. Doing so may not utilize the maximum chip width for the MRR, but the quick selection and guarantee of stability are still valuable in applications, especially in small machine shops. The upper border line can also provide a quick check for instability, so that we can avoid the cuttings where chip width falls into the unconditionally unstable region.

4.3 The optimum chip width at sweet spots

All lobes intersect with other lobes on both sides, except for the #0 lobe which has no intersection point with other lobes on its right side. The intersection points are the peak points of the lobes, and they provide the deepest cuts at various speed ranges nearby. Therefore, these

peak points are called the sweet spots. If we could locate these sweet spots or the optimum depths of cut, we will be able to fully utilize the potential of the machining system and obtain the most efficient material removal rate (MRR). A method is introduced here to analytically determine the approximate sweet spots at the intersections.

The sweetest spot is the intersection of the #0 lobe and #1 lobe, which provides the deepest cut at the highest spindle speed. Due to many other factors, such as the limits of machine power and spindle speed, it may not be practical to operate a specific machine to cut certain workpiece materials at the sweetest spot.

5. The optimum chip widths

5.1 Difficulties in determining the optimum chip widths

In the past, the optimum chip widths or sweet spots were approximately interpolated read by eye from the stability lobe diagram at the intersections of the lobes. This graphical solution neither utilizes available modern computing power nor provides accurate and consistent numerical values.

Researchers have made efforts to calculate the optimum chip widths. Based on the resonance of frequencies, Smith and Tlusty [6] suggested that the maximum chip widths occur when the tooth frequency f_t (or a multiple of tooth frequencies) matches the natural frequency f_n,

$$f_n = (n + 1)f_t \quad or \quad r_t = f_t / f_n = 1 / (n + 1), \quad n = 0, 1, 2, \ldots \tag{11}$$

where the maximum chip width occurs at the intersection of the n^{th} lobe and the $(n + 1)^{th}$ lobe. Eq. 11 gives results of $r_t = f_t / f_n = 1, 1/2, 1/3, \ldots$ for the consecutive series of lobes. From the stability lobe diagram (Figure 2), these values on the x-axis correspond to the vertical asymptotes at the left branches of the lobes. At these points, the chip widths are infinite.

Smith & Tlusty [6] also made an attempt to relate the chatter frequency f to the tooth frequency f_t. They suggested that the peak point between the n^{th} lobe and the $(n + 1)^{th}$ lobe may be found by the intersection of two functions. One of them is the chatter frequency function f for the n^{th} lobe, and the other is the tooth frequency function $(n + 1)f_t$, both as function of the tooth frequency f_t (Figure 3). The tooth frequency function $(n + 1)f_t$ is a simple linear function with expressions of f_t, $2f_t$, $3f_t$, … for the lobes #0, #1, #2, etc. At the intersection points of the two functions, we have

$$f = (n + 1)f_t \quad or \quad r = (n + 1)r_t, \quad n = 0, 1, 2, \ldots \tag{12}$$

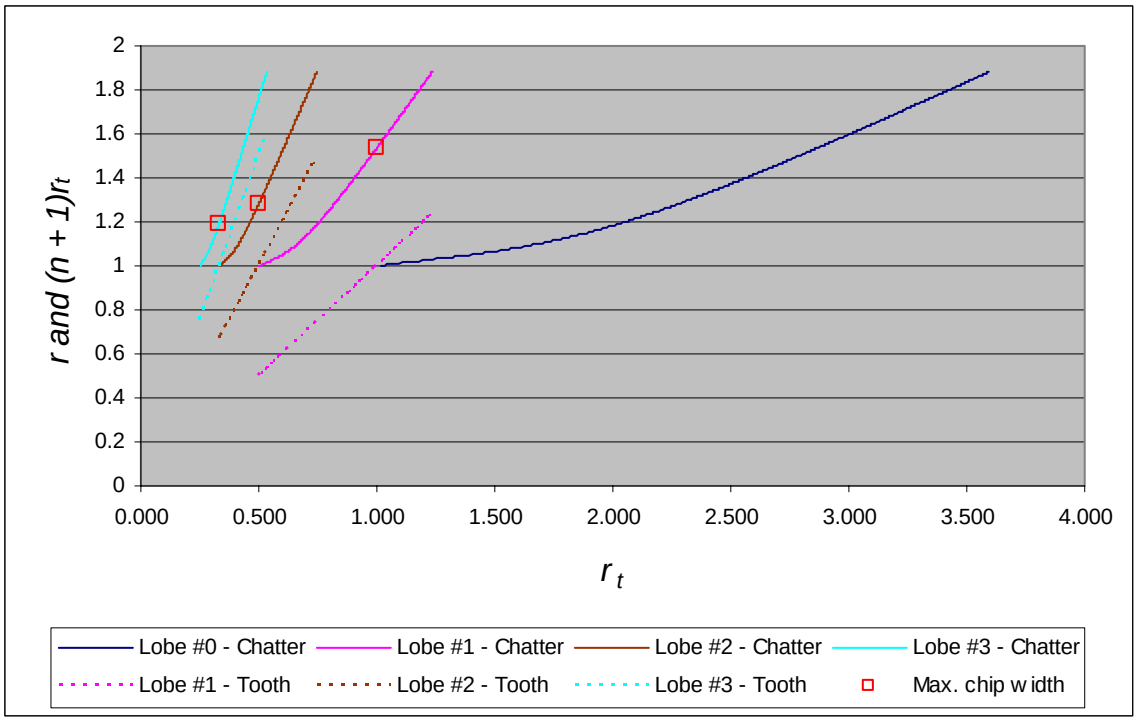

Figure 3 Approximate locations of the optimum chip widths

This approach does not work either. Comparing Figure 3 with Figure 2, we see these intersection points also correspond to the vertical asymptotes at the left branches of the lobes, resulting in infinite chip widths.

Why do both approaches encounter the same difficulty of yielding infinite chip widths? The cause may be the attempt to relate the three frequencies: chatter frequency f, natural frequency f_n, and tooth frequency f_t through eq. 7, eq. 11, and eq. 12.

Letting $\varepsilon = 2\pi$ in eq. 7 produces eq. 12. However, when $\varepsilon = 2\pi$, there is no phase shift between the chatter frequency f and tooth frequency f_t. This means that the chatter frequency is equal to the tooth frequency by a factor of $(n + 1)$. When this happens, the two frequencies are in harmony. This situation violates the fundamental assumption of regenerative chatter theory: the chatter is caused by the phase shift between the surface waviness of consecutive cuts.

If we let $\varepsilon = 0$ and $f = f_n$ in eq. 7, we obtain eq. 11. Not only is zero phase shift ($\varepsilon = 0$) is not allowed by the regenerative chatter theory, but also the chatter frequency f cannot be equal to the natural frequency f_n. The point at $r = f / f_n = 1$ is a singular point, which makes the real FRF $Gr = 0$ (eq. 4), and as a result, $b = \infty$ (eq. 3). This condition results in the vertical asymptotes at the left branches of the lobes.

5.2 Approximate solution of the optimum chip widths

Thus far, we have not been able to solve for the intersection points of the lobes. A method is introduced here to analytically calculate the approximate optimum chip widths. It also provides a procedure of finding the sweet spots using a spreadsheet.

Let us look again at the relationship between the chatter frequency f and the tooth frequency f_t (or $r = f / f_n$ and $r_t = f_t / f_n$). We know from eq. 11 that when r_t = 1, 1/2, 1/3, … , the vertical asymptotes exist at the left branches of the lobes in the stability lobe diagrams. At these locations, the chip widths are infinite. However, we may still use the relationship to analytically locate the approximate peak values of the chip widths or the intersections of the lobes. Figure 4 shows both relationships of $r \sim r_t$ and $(n + 1)r_t \sim r_t$. At each value of $(n + 1)r_t$ on the x-axis, there are two corresponding values of r, r_n and r_{n+1}, on the y-axis for any pair of adjacent lobes n and $(n + 1)$. The values of r_n from the n^{th} lobe approach 1, which yields $r_b = \infty$, therefore, not applicable. However, the value of r_{n+1} from the next $(n + 1)^{th}$ lobe is finite, which may be used to determine the intersection points of the n^{th} and $(n + 1)^{th}$ lobes, i.e., the optimum depths of cut b (or r_b), with very close approximations. These points are marked in Figure 3 as squares on the $r \sim r_t$ plots.

The idea of calculating the approximate optimum chip width is actually quite simple. Since the suggested intersection points (eq. 11 and eq. 12) are invalid with infinite chip widths for the n^{th} lobe, we will use the same value on the x-axis to calculate the chip width for the $(n + 1)^{th}$ lobe, and obtain the result as an approximate intersection point for the n^{th} and $(n + 1)^{th}$ lobes, The governing equations and detailed procedures to calculate the intersection points are as follows.

The approximate intersection point for the n^{th} lobe and $(n + 1)^{th}$ lobe is located at the point on the x-axis:

$$r_t = \frac{1}{n+1}, \quad n = 0, 1, 2, \ldots \tag{13}$$

For the $(n + 1)^{th}$ lobe, from eq. 9, we have

$$r_t = \frac{r}{n+1+\frac{1}{2}+\frac{1}{\pi}\tan^{-1}\frac{-2\zeta r}{1-r^2}}, \quad n = 0, 1, 2, \ldots \tag{14}$$

Substituting eq. 13 into eq. 14, we obtain

$$\frac{r}{n+1+\frac{1}{2}+\frac{1}{\pi}\tan^{-1}\frac{-2\zeta r}{1-r^2}}=\frac{1}{n+1},\quad n = 0, 1, 2, \ldots \tag{15}$$

Solve eq. 15 for r. Substituting r into eq. 6, we obtain the approximate optimum chip width b (or r_b).

It may require multiple iterations to solve eq. 15 numerically. It is convenient to use a spreadsheet to calculate the approximate optimum chip width r_b (Table 2). A step-by-step procedure of the calculations is illustrated in Table 2 as an example. In order to compare the results, the same data [4] used to create Figure 1 are used here again. The chip width value for each n is the approximate intersection point between the n^{th} lobe and $(n + 1)^{th}$ lobe. Both the dimensionless relationship of $r_t \sim r_b$ and the dimensional relationship $N \sim b$ are listed in the table for comparison.

Table 2 Calculated optimum chip widths

n	r_t	r	r_b	N	b
0	1.000	1.536	6.555	15,002	6.883
1	0.500	1.282	3.186	7,504	3.345
2	0.333	1.195	2.197	4,998	2.307
…	…	…	…	…	…

Step 1. For lobe number n, calculate r_t from eq. 13.
Step 2. Also for lobe number n, calculate r by iteration from eq. 15.
Step 3. Substitute r into eq. 9 to obtain r_b.
Step 4. The result of r_b is the approximate optimum chip widths at r_t. for the intersection of the n^{th} and $(n + 1)^{th}$ lobes. The results may also be written as the spindle speed vs. chip width $N \sim b$.

The calculated approximate analytical solutions of the intersections (Table 2) are plotted in Figure 2, and marked by square symbols. The intersection values interpolated by graphic solutions (also approximate) from Figure 1 are also listed in Tale 3 for comparison with the approximate analytical solutions in Table 2. From Figure 2 and the comparison of the data in Table 2 and Table 3, the calculated approximate points are located to the left of the "actual" intersections. The differences of the optimum chip widths (b or r_b) between the analytical calculations (Table 2) and the interpolated graphic solutions (Table 3) are closer in absolute values toward lower spindle speeds, while smaller in relative variations toward higher spindle speeds. At the sweetest spot or the intersection of the #0 lobe and #1 lobe, the difference of r_b is 0.575 or 8%. Therefore, the method can be used to analytically calculate a good approximation of optimum chip widths for MRR.

Table 3 Graphic solution of optimum chip widths

n	r_t	r	r_b	N	b
0	1.027	1.536	7.130	15,404	7.487
1	0.515	1.282	3.598	7,721	3.778
2	0.344	1.195	2.583	5,161	2.712
…	…	…	…	…	…

6. Conclusion

A method of using a spreadsheet to create stability lobe diagrams is presented. This step-by-step procedure provides an easy way for machine operators to choose the optimum chip widths and high spindle speeds at the sweet spots on the diagram to obtain a high material removal rate (MRR). It also helps students to understand the theory of machine chattering, and practice on the optimum cutting parameters in machining processes. A stability lobe diagram is composed of a series of scallop-shaped chatter lines. It may be represented either as the relationship between the chip width or depth of cut and spindle speed as $b \sim N$, or as a dimensionless relationship between the ratios of the chip width to the minimum chip width and the tooth-stroke frequency to the natural frequency as r_b and r_t. The dimensionless relationship is preferable because it makes it easy to compare machining processes under different cutting parameters and conditions.

The intersections or sweet spots of the consecutive series of lobes provide the optimum chip widths. In the past, the sweet spots were found by graphic solutions from the stability lobe diagram. An analytical method is presented here to calculate the approximate optimum chip widths. A step-by-step procedure for doing the calculation using a spreadsheet is also presented. The results of the method show that they are close to the actual values, especially for the sweetest spot at the intersection of the #0 lobe and #1 lobe, which provides the stable machining at the highest spindle speed and the deepest depth of cut. The method may be used to easily obtain a quick estimate of the optimum chip widths for calibrating the cutting parameters.

The figures and tables were created using the same data as the example by Tlusty [4] for verifications of the methods and comparisons of results. They showed that the methods yielded outcomes very similar to Tlusty's results. Machining is a very complicated process. There are many parameters that contribute to the interactions between machine tool, cutting tool, and workpiece. For example, additional factors must be considered in milling processes, such as the interrupted cutting process caused by multi-tooth cutters, the variable chip width from the entry to the exit of a cuter tooth, and the variable directions of cutting force with respect to a fixed coordinate system. More complications also arise in multiple degrees of freedom in multi-mode machine chattering. Due to the limit of the scope, we have only discussed the fundamental

concepts and procedures in creating a stability lobe diagram. More discussion of the regenerative chatter theory and the stability lobe diagram will be presented in the future.

7. Acknowledgements

This paper is a partial result of the author's one year research residence in 2003-2004 at the NASA Langley Research Center in Hampton, Virginia as a NASA Administrator's Fellow, with funding from the NASA Administrator's Fellowship Program (NAFP). The NAFP program is administered by the United Negro College Fund Special Programs Corporation (UNCFSP).

Bibliography

[1] DeGarmo, E. P., Black, J. T., & Kohser, R. A. *Materials and Processes in Manufacturing*. 9th ed., 2003 by John Wiley & Sons, Inc.

[2] Tobias, S. A. & Fishwick, W. Theory of regenerative machine tool chatter. *The Engineer, London,* Vol. 205, 1958, 199-203 (Feb. 7), 238-239 (Feb. 14).

[3] Merritt, H. E. Theory of self-excited machine-tool chatter - Contribution to machine-tool chatter research – 1. *ASME J. Eng. for Ind.*, 87, November 1965, 447-454.

[4] Tlusty, J. Machine Dynamics. *Handbook of High Speed Machining Technology.* King, R. I., ed., 1985, Chapman and Hall, New York, Ch. 3, 48-153.

[5] Tlusty, J. Dynamics of high-speed milling. *J. of Engineering for Industry, Trans. ASME*, 108, May 1986, 59-67.

[6] Smith, S. & Tlusty, J. Update on high-speed milling dynamics. *J. Engineering for Industry, Trans. ASME*, 112, May 1990, 142-149.

[7] Altintas, Y. & Budak, E. Analytical prediction of stability lobes in milling. *Ann. CIRP*, 44(1), 1995, 357-362.

[8] Mann, B. P. *Dynamic models of milling and broaching*. Doctor of Science Dissertation, Washington Univ., Saint Louis, Missouri, May, 2003.

[9] Rao, B. *Modeling and analysis of high speed machining of aerospace alloys*. Ph.D. Thesis, Purdue Univ., Aug. 2002.

[10] Wang, Z. *Chatter analysis of machine tool systems in turning processes*. Ph.D. Thesis, Univ. of Toronto, Canada, 2001.

[11] Zhao, M. *Dynamics and stability of milling processes*. Ph.D. Dissertation, Univ. of Maryland, 2000.

[12] Li, C. –J. *Tool-tip displacement measurement, process modeling, and chatter avoidance in agile precision line boring*. Ph.D. Thesis, Univ. of Michigan, 1999.

[13] Jaganathan, V. *A study of the dynamics of drilling and reaming*. Ph.D. Thesis, Univ. of Windsor, Canada, 1998.

[14] Tian, J. *Self-excited vibration of rotating discs and shafts with applications to sawing and milling*. Ph.D. dissertation, The Univ. of British Columbia, Canada, August 1998.

[15] Balan, A. *Theoretical and experimental investigations on radial electromagnetic forces in relation to vibration problems of induction machines*. Ph.D. Thesis, Univ. of Saskatchewan, Canada, June 1997.
[16] El-Mounayri, H. A. *Generic solid modeling based machining process simulation*. Ph.D. Thesis, McMaster Univ., Canada, June 1997.
[17] Fraser, S. *Multi-variable optimal numerical control using adaptive model for identification of thermally induced deformation in high-speed machine tools*. Ph.D. Thesis, Concordia Univ., Canada, Aug. 1997.
[18] Gadalla, M. *Improving the accuracy of parametric surfaces using cutting force synthesis and surface offset techniques*. Ph.D. Thesis, Univ. of Western Ontario, Canada, Oct. 1997.
[19] Pratt, J. R. *Vibration control for chatter suppression with application to boring bars*. Ph.D. Dissertation, Virginia Polytechnic Inst. & State Univ., Nov. 1997.
[20] Jayaram, S. *Stability and vibration analysis of turning and face milling processes*. Ph.D. thesis, Univ. of Illinois at Urbana-Champaign, 1996.
[21] Liasi, E. *Surface finish enhancement in a turning operation via control of the depth of cut*. Ph.D. Thesis, Univ. of Windsor, Canada, 1996.
[22] Budak, E. *Mechanics and dynamics of milling thin walled structures*. Ph.D. Thesis, The Univ. of British Columbia, Vancouver, B.C., Canada, 1994.
[23] Bayly, Philip V. *Measurements of instability and disorder in nonlinear mechanical and cardiac oscillations*. Ph.D. Dissertation, Duke Univ., 1993.
[24] Fofana, M. S. *Delay dynamical systems with applications to machine-tool chatter*. Ph.D. Thesis, Univ. of Waterloo, Canada, 1993.
[25] Dohner, J. L., et al. Mitigation of chatter instabilities in milling by active structural control. *J. Sound & Vibration*, 269, 2004, 197-211.
[26] Merdol, S. D. & Altintas, Y. Mechanics and dynamics of serrated cylindrical and tapered end mills. *Trans. ASME, J. Manuf. Sci. Eng.*, 126, 2004, 317-326.
[27] Amin, A. & Abdelgadir, M. The effect of preheating of work material on chatter during end milling of medium carbon steel performed on a vertical, machining center. *J. Manufacturing Science & Engineering*, 125, Nov. 2003, 674-680.
[28] Bayly, P. V., et al. Stability of interrupted cutting by temporal finite element analysis. *ASME J. Manuf. Sci. Eng.*, 125, 2003, 220-225.
[29] Budak, E. An analytical design method for milling cutters with nonconstant pitch to increase stability, Part I: Theory. *J. Manufacturing Science & Engineering, Trans. ASME*, 125, Feb. 2003, 29-34.
[30] Budak, E. An analytical design method for milling cutters with nonconstant pitch to increase stability, Part II: Application. *J. Manufacturing Science & Engineering, Trans. ASME*, 125, Feb. 2003, 35-38.
[31] Choi, T. & Shin, Y. On-line chatter detection using wavelet-based parameter estimation. *J. Manufacturing Science & Engineering*, 125, Feb. 2003, 21-28.
[32] Faassen, R. P. H., van de Wouw, N., Oosterling, J. A. J., & Nijmeijer, H. Prediction of regenerative chatter by modeling and analysis of high-speed milling. *Int. J. Mach. Tools Manuf.*, 43, 1437-1446, 2003.

[33] Fofana, M. S. Delay dynamical systems and applications to nonlinear machine-tool chatter. *Chaos, Solitons and Fractals*, 17(4), 2003, 731-747.
[34] Insperger, T., Stepan, G., Bayly, P. V., & Mann, B. P. Multiple chatter frequencies in milling processes. *J. Sound & Vibration*, 262, 2003, 333-345.
[35] Insperger, T., Stepan, G., Bayly, P. V., & Mann, B. P. Multiple chatter frequencies in milling processes. *J. Sound & Vibration*, 262, 2003, 333-345.
[36] Li, C. -J., Ulsoy, A. G., & Endres, W. J. The effect of flexible-tool rotation on regenerative instability in machining. *ASME J. Manuf. Sci. Eng.*, 125, 2003, 39-47.
[37] Li, H., Li, X., & Chen, X. A novel chatter stability criterion for the modeling and simulation of the dynamic milling process in the time domain. *Int. J. Advanced Manuf. Technology*, 22(9-10), 2003, 619-625.
[38] Schmitz, T. L. Chatter recognition by a statistical evaluation of the synchronously sampled audio signal. *J. Sound & Vibrations*, 262, 2003, 721-730.
[39] Schmitz, T., Burns, T. Receptance Coupling for High-Speed Machining Dynamics Prediction. *Proceedings of the 2003 International Modal Analysis Conference (IMAC-XXI)*, February 3-6, 2003, Kissimmee, FL.
[40] Warminski, J. et al. Approximate analytical solutions for primary chatter in the non-linear metal cutting. *J. Sound & Vibration*, 259(4), 2003, 917-933.
[41] Bayly, P. V., et al. Effects of radial immersion and cutting direction on chatter instability in end-milling. *Proc. Int. Mech. Eng. Conf. & Exp. (IMECE 2002)*, New Orleans, LA, Nov. 17-22, 2002.
[42] Endres, W. & Loo, M. Modeling cutting process nonlinearity for stability analysis – Application to tooling selection for valve-seat machining. *5th CIRP Int'l Workshop on Modeling of Machining*, May 2002, 71-82.
[43] Fofana, M. S. Aspects of stable and unstable machining by Hopf bifurcation. *Applied Mathematical Modelling,* 26(10), October 2002, 953-973.
[44] Fofana, M. S. Sufficient conditions for the stability of single and multiple regenerative chatter. *Chaos, Solitons and Fractals*, 14, 2002, 335-347.
[45] Lange, J. H. & Abu-Zahra, N. H. Tool chatter monitoring in turning operations using wavelet analysis of ultrasound waves. *Int'l J. Adv. Manuf. Technology*, 20(4), Aug., 2002, 248-254.
[46] Schmitz, T. L. Automatic trimming of machining stability lobes. *Int. J. Machine Tools & Manufacture*, 42(13), 2002, 1479-1486.
[47] Schmitz, T., Medicus, K., Dutterer, B. Exploring Once-per-revolution Audio Signal Variance as a Chatter Indicator. *Machining Science and Technology*, 6(2), 2002, 207-225.
[48] Bayly, P. V., et al. Analysis of tool oscillation and hole roundness error in a quasi-static model of reaming. *J. Manuf. Sci. Eng.*, 123(3), 2001, 387-396.
[49] Bayly, P. V., et al. Theory of torsional chatter in twist drills: model, stability analysis and composition to test. *J. Manuf. Sci. Eng.*, 123(4), 2001, 552-561.
[50] Engin, S. and Altintas, Y. Mechanics and dynamics of general milling cutters, Part I: Helical end mills. *Int. J. Mach. Tools Manuf.*, 41(15), 2001, 2195-2212.

[51] Engin, S. and Altintas, Y. Mechanics and dynamics of general milling cutters, Part II: Inserted cutters. *Int. J. Mach. Tools Manuf.*, 41(15), 2001, 2213-2231.
[52] Schmitz, T. L., Davies, M. A., & Kennedy, M. D. Tool point frequency response prediction for high-speed machining by RCSA. *Journal of Manufacturing Science and Engineering, Trans. ASME,* 123, November 2001, 700-707.
[53] Schmitz, T. L., et al. Improving high-speed machining material removal rates by rapid dynamic analysis. *Annals of the CIRP*, 50(1), 2001, 263-268.
[54] Wang, M. & Fei, R. On-line chatter detection and control in boring based on an electrorheological fluid. *Mechatronics*, 11(7), 2001, 779-792.
[55] Bao, W. and Tanselm I. Modeling micro-end-milling operations, Part I: Analytical cutting force model, *Int. J. Mach. Tools Manuf.*, 40(15), 2000, 2155-2173.
[56] Bao, W. and Tanselm I. Modeling micro-end-milling operations, Part II: Tool run-out, *Int. J. Mach. Tools Manuf.*, 40(15), 2000, 2175-2192.
[57] Bao, W. and Tanselm I. Modeling micro-end-milling operations, Part III: Influence of tool wear, *Int. J. Mach. Tools Manuf.*, 40(15), 2000, 2193-2211.
[58] Fofana, M. S. On the stationary stability of machine-tool chatter with ergodic damping process. *8th ASCE Specialty Conf. on Probabilistic Mechanics and Structural Reliability*, PMC2000-265.
[59] Insperger, T. & Stepan, G. Stability of high-speed milling. *Proc. Symp. Nonlinear & Stochastic Mechanics*, Orlando, FL, 2000, AMD Vol. 241, pp. 119-123.
[60] Jayaram, S., Kapoor, S. G., & DeVor, R. E. Analytical stability analysis of variable spindle speed machining. *J. Manufacturing Science & Engineering, Trans. ASME*, 122, Aug. 2000, 391-397.
[61] Schmitz, T. L. Predicting high-speed machining dynamics by substructure analysis. *Annals of the CIRP*, 49(1), 2000, 303-308.
[62] Altintas, Y., Engin, S., & Budak, E. Analytical stability prediction and design of variable pitch cutters. *J. Manufacturing Science & Engineering, Trans. ASME*, 121(2), 1999, 173-178.
[63] Altintas, Y., Shamoto, E., Lee, P., & Budak, E. Analytical prediction of stability lobes in ball end milling. *J. Manufacturing Science & Engineering, Trans. ASME*, 121(4), 1999, 586-592.
[64] Jensen, S. & Shin, Y. Stability analysis in face-milling operations, Part I: Theory of stability lobe prediction. *ASME J. Manuf. Sci. Eng.*, 21(4), 1999, 600-605.
[65] Jensen, S. & Shin, Y. Stability analysis in face-milling operations, Part II: Experimental validation and influencing factors. *ASME J. Manuf. Sci. Eng.*, 21(4), 1999, 606-614.
[66] Rao, B. C. & Shin, Y. C. A comprehensive dynamic cutting force model for chatter prediction in turning. *Int. J. Mach. Tools Manuf.*, 39, 1999, 1531-1654.
[67] Schmitz, T., Ziegert, J. Examination of Surface Location Error Due to Phasing of Cutter Vibrations. *Precision Engineering,* 23(1), January 1999, 51-62.
[68] Budak, E. & Altintas, Y. Analytical prediction of chatter stability in milling-Part I: General formulation. *J. Dynamic Systems, Measurement, and Control, Trans. ASME*, 120, 1998, 22-30.

[69] Budak, E. & Altintas, Y. Analytical prediction of chatter stability in milling-Part II: Application of the general formulation to common milling systems. *J. Dynamic Systems, Measurement, and Control, Trans. ASME*, 120, 1998, 31-36.
[70] Endres, W. J. A Quantitative Energy-Based Method for Predicting Stability Limit as a Direct Function of Spindle Speed for High-Speed Machining. *Trans. of NAMRI/SME*, 24, 1996, 27-32.
[71] Wang, J. H. & Lee, K. N. Suppression of chatter vibration of a CNC machine centre – an example. *Mech. Sys. & Signal Processing*, 10(5), 1996, 551-560.
[72] Jemielniak, K. & Widota, A. Suppression of self excited vibration by the spindle speed variation method. *Int. J. Mach. Tool. Des. Res.*, 24(3), 1994, 207-214.
[73] Weck, M., Altintas, Y., & Beer, C. CAD assisted chatter-free NC tool path generation in milling. *Int. J. Mach. Tool Des. Res.*, 34(6), 1994, 879-891.
[74] Minis, I. & Yanushevsky, R. A new theoretical approach for prediction of stability lobes in milling. *ASME J. Eng. For Ind.*, 115, Feb. 1993, 1-8.
[75] Smith, S. & Tlusty, J. Efficient simulation programs for chatter in milling. *Annals of the CIRP*, 42(1), 1993, 463-466.

Biography

JIANPING YUE is a Professor and the Chairperson of the Division of Engineering Technologies and Computer Sciences at Essex County College, Newark, New Jersey. He is a NASA Administrator's Fellow, and a Certified Senior Industrial Technologist by the National Association of Industrial Technology. Dr. Yue received his B.S. and M.S. degrees in Hydraulic and Coastal Engineering from Wuhan University, China in 1977 and 1982, and a Ph.D. degree in Civil Engineering from the University of Memphis, Tennessee in 1990.